Journal of Geophysical Research: Biogeosciences

RESEARCH ARTICLE
10.1029/2017JG004310

Special Section:
Extreme Climate Event Impacts on Aquatic Biogeochemical Cycles and Fluxes

High-Frequency Sensor Data Reveal Across-Scale Nitrate Dynamics in Response to Hydrology and Biogeochemistry in Intensively Managed Agricultural Basins

Amy Hansen[1,2] **and Arvind Singh**[3]

[1]St Anthony Falls Laboratory, College of Science and Engineering, University of Minnesota, Minneapolis, MN, USA, [2]Now at Department of Civil, Environmental and Architectural Engineering, University of Kansas, Lawrence, KS, USA, [3]Department of Civil, Environmental, and Construction Engineering, University of Central Florida, Orlando, FL, USA

Key Points:
- Discharge, nitrate concentration, and temperature exhibited power law behavior with similar slopes for eight agricultural watersheds in Iowa
- Cross correlation between nitrate and discharge increased with watershed area, yet peaks were not temporally aligned
- Multiscale nitrate temporal behavior was significantly related to watershed area, geology, and land use

Correspondence to:
A. Hansen,
amy.hansen@ku.edu

Citation:
Hansen, A., & Singh, A. (2018). High-frequency sensor data reveal across-scale nitrate dynamics in response to hydrology and biogeochemistry in intensively managed agricultural basins. *Journal of Geophysical Research: Biogeosciences*, *123*, 2168–2182. https://doi.org/10.1029/2017JG004310

Received 14 NOV 2017
Accepted 6 JUN 2018
Accepted article online 15 JUN 2018
Published online 20 JUL 2018

Abstract Excess nitrate in rivers draining intensively managed agricultural watersheds has caused coastal hypoxic zones, harmful algal blooms, and degraded drinking water. Hydrology and biogeochemical transformations influence nitrate concentrations by changing nitrate supply, removal, and transport. For the Midwest Unites States, where much of the land is used for corn and soybean production, a better understanding of the response of nitrate to hydrology and biogeochemistry is vital in the face of high nitrate concentrations coupled with projected increases of precipitation frequency and magnitude. In this study, we capitalized on the availability of spatially and temporally extensive sensor data in the region to evaluate how nitrate concentration (NO_3^-) interacts with discharge (Q) and water temperature (T) within eight watersheds in Iowa, United States, by evaluating land use characteristics and multiscale temporal behavior from 5-year, high-frequency, time series records. We show that power spectral density of Q, NO_3^-, and T, all exhibit power law behavior with slopes greater than 2, implying temporal self-similarity for a range of scales. NO_3^- was strongly cross correlated with Q for all sites and correlation increased significantly with drainage area across sites. Peak NO_3^- increased significantly with crop coverage across watersheds. Temporal offsets in peak NO_3^- and peak Q, seen at all study sites, reduced the impact of extreme events. This study illustrates a relatively new approach to evaluating environmental sensor data and revealed characteristics of watersheds in which extreme discharge events have the greatest consequences.

Plain Language Summary Nitrate export from the Midwest United States has caused water quality degradation extending from the Midwest, where concentrations exceed drinking water limits, to the northern Gulf of Mexico, where it contributes to the formation of the Dead Zone. Climate models predict that precipitation in the Midwest will increase; therefore, understanding the response of nitrate to streamflow (discharge) is vital. In this study, we analyzed the patterns within nitrate, discharge and temperature sensor data over time for eight agricultural watersheds to determine how nitrate concentration is related to discharge or water temperature. From this, we evaluated the relative importance of hydrology vs. nitrate removal or release in controlling nitrate export. We show that nitrate, discharge, and temperature all exhibit self-similar characteristics across a range of temporal scales and that the percent of land used for agriculture was predictive of peak nitrate concentration. We found that nitrate was strongly related to discharge and that the similarity between nitrate and discharge increased with watershed size. However, peak nitrate concentration generally lagged behind peak discharge resulting in maximum peak nitrate loads often occurring at intermediate-sized, not extreme, events.

1. Introduction

The Midwestern United States is often referred to as the Corn Belt for its importance as a center of agriculture. In this region, high crop productivity is achieved through the implementation of intensive landscape management practices including subsurface tile drainage and high fertilization rates (Blann et al., 2009; Tilman et al., 2002). Nitrogen inputs, largely from fertilizer application, are estimated to be 10–15 times higher than the turn of the twentieth century (Galloway et al., 2004; Howarth et al., 2012). In the Corn Belt, an estimated 50% of applied nitrogen is not assimilated by crops but either stored within soils or lost to the riverine network (Howarth et al., 2012). Despite stable nitrogen input rates since the 1980s (McIsaac et al.,

2002; Randall & Mulla, 1995), flow-normalized annual nitrate concentration and flux in the Mississippi River have continued to rise over the same time period (Sprague et al., 2011). The increased nitrate flux may be due to increases in fertilized land area as crop production has expanded to meet the demands of the ethanol market (Lark et al., 2015), or to legacy accumulation of nitrogen within the soil and groundwater (Basu et al., 2010; Sebilo et al., 2013; Sudduth et al., 2013; Van Meter et al., 2016). Because groundwater and soil stores of nitrogen are significant, watershed scale analyses are likely required to interpret spatial and temporal patterns in nitrate concentration and loading.

Midwestern agricultural productivity has come at the expense of the water quality and ecological integrity of local and downstream surface water, most notably the Northern Gulf of Mexico (David et al., 2010; Goolsby et al., 2000). Nitrate losses from the Corn Belt during spring have been shown to correlate well with the peak size of the northern Gulf of Mexico hypoxic zone (Howarth & Marino, 2006; Rabalais et al., 2002; Turner et al., 2008). Within the seasonally occurring Northern Gulf of Mexico hypoxic zone, an area that averaged 15,900 km^2 between 1993 and 2005, prolonged low-oxygen concentrations result in mass die-offs of sessile or slow-moving fauna and regional evacuation by fish (Diaz & Rosenberg, 2008; Rabalais et al., 2007). Northern Gulf of Mexico hypoxia is anticipated to worsen in the future due to projected increases in precipitation frequency and magnitude and subsequent projected increases in nitrate loading from the Corn Belt (Sinha et al., 2017). Local consequences of high nitrate include health impairments for human consumption and population loss for aquatic fauna (Vitousek et al., 1997; Wagenhoff et al., 2017).

Our understanding of controls on riverine nitrate is hindered by an incomplete understanding of the role of hydrology versus biogeochemistry on NO_3^- release and transport within these landscapes. NO_3^- data, observed at one location within a river, integrate information about nitrogen input, storage, transformation, and transport processes occurring on the land and stream, and in groundwater that drains into that location. In agricultural landscapes, this is further complicated by varying scales of spatial connectivity and temporal alignments of processes acting upon nitrogen such as nitrogen transformation and delivery, precipitation and snowmelt seasonality, crop fertilization timing, and hydrologic routing (e.g., Dubrovsky et al., 2010). Legacy stores of excess nitrogen in soils and groundwater of agricultural watersheds, often in the form of organic nitrogen, complicate the problem by providing an additional internal source and have a long-term effect on nitrate dynamics (Van Meter et al., 2016). Furthermore, the watershed and the river network structure organize discharge such that magnification or lessening of NO_3^- concentrations can occur depending on the topological organization of the channel network (Helton et al., 2017). Due to the spatial and temporal complexity of this problem, an approach is needed that incorporates a broad range of information into the analysis.

In the most heavily farmed regions of the Upper Mississippi River basin, high-frequency nitrate sensors have been colocated at discharge gaging sites in order to capture more information about the interactions between nitrate and potential controls on its export including discharge and temperature (https://waterdata.usgs.gov/nwis). To date, these data have been used largely to explore nitrate load timing, rate, and magnitude and thus prediction capabilities for downstream environmental consequences (Jones et al., 2017; Pellerin et al., 2012, 2014). To our knowledge, across-scale nitrate process dynamics have not been systematically investigated in heavily agriculturally managed landscapes, although some work has occurred in less impacted watersheds (Aubert et al., 2016; Downing et al., 2017). This is, in part, because the high-frequency nitrate data generated from these sensors are only recently long enough to use frequency analysis tools on, such as spectral analysis among others, to extract information about the signature of different processes on change in variability in NO_3^- across a range of scales.

In this study we investigated whether the relative contribution of hydrology and biogeochemistry toward nitrate regulation was evident in across-scale patterns in NO_3^- dynamics. We used simultaneously sampled nitrate, discharge, and temperature measurements collected at 15-min intervals for approximately 5 years from eight intensively managed agricultural watersheds within the Corn Belt. Study watershed areas ranged from 520 to 32,300 km^2 and were intensively cultivated for corn and soybean production. Our first hypothesis is that the relative importance of hydrological and biogeochemical processes toward NO_3^- export can be extracted from multiscale temporal NO_3^-, Q, and T statistics. We use discharge as an indicator of hydrologic activity and temperature as a surrogate for in-channel biogeochemical activity due to its strong effect on metabolism and productivity (Wetzel, 2001). Dissecting these signals into the processes that are ultimately controlling nitrate export could provide insight into where and when nitrogen management efforts would be most effective. Second, we ask if nitrate multiscale response characteristics can be used to constrain the estimated

Table 1
Summary of Measurement Locations, Drainage Area Characteristics, and Percent Missing From Data Used in Spectral Analysis

Site #	Site name	Station	Drainage area (km^2)	>50% karst geology	Latitude/ longitude	Land use (%)					% Missing data		
						WL	CL	DEV	FOR	GRS	*Q*	NO_3	*T*
1	Old Man's Creek	5455100	521	Yes	41.6064, −91.6157	1.6	62.4	7.1	2.7	26.2	0.4	30.5	N/A
2	North Raccoon River-Sac City	5482300	1,813	No	42.3544, −94.9908	2.1	87.6	7.1	0.3	2.9	17.8	14.0	1.7
3	North Raccoon River-Jefferson	5482500	4,193	No	41.9880, −94.3769	2.3	85.8	6.9	0.8	4.1	16.8	31.8	10.2
4	Raccoon River-Van Meter	5484500	8,912	No	41.5339, −93.9500	2.1	79.4	6.8	3.2	8.4	18.1	16.1	10.2
5	Iowa River	5465500	32,375	Yes	41.1781, −91.1821	3.2	73.4	8.7	3.3	11.4	3.7	31.8	N/A
6	Boone River	5481000	2,186	Yes	42.4325, −93.8058	1.7	88.8	6.8	0.2	2.5	22.5	41.2	20.5
7	Des Moines River	5482000	16,174	No	41.6125, −93.6211	3.4	82.2	7.4	2.4	4.6	12.7	10.9	1.0
8	Cedar River	5464420	16,426	Yes	42.0692, −91.7852	3.1	78.5	8.6	2.1	7.6	13.4	31.8	10.9

Note. Abbreviations for land use are WL for wetlands and lakes, CL for cropland, DEV for developed land, FOR for forested land cover, and GRS for grasslands including prairie and pasture. N/A = not applicable.

magnitude of NO_3^- export in response to anticipated increases in frequency and magnitude of extreme discharge events. Our second hypothesis is that the magnitude of NO_3^- export under extreme discharge conditions can be determined through analysis of NO_3^- and *Q* time series data. A better understanding of the effect of extreme events on nitrate export and how that varies between watersheds could enable society to better prepare for such events. Together, this analysis contributes toward our collective understanding of landscape controls on nitrate release dynamics and the implications of extreme discharge events.

2. Data and Methods

2.1. Site Description

We focus our analysis on sensor data from eight riverine locations within Iowa, United States (Table 1). These sites were chosen to span a large range in contributing drainage area with predominantly agricultural land use and to have 5 years of sensor data available for nitrate concentration (NO_3^-, mg/L), discharge (*Q*, m^3/s), and temperature (*T*, °C) with minimal nonseasonal breaks in the record. In some cases, site watersheds are nested. Two sites were identified as being located downstream of a flow-regulation structure: Des Moines River and Iowa River. The Des Moines River site was immediately downstream of a large reservoir where flow is actively controlled. Contributing drainage areas (i.e., watersheds) for individual sites range from 520 to 32,300 km^2. Together, the eight sites cover a nonoverlapping area of 73,000 km^2, or slightly larger than the country of Ireland.

Watersheds for the study sites are primarily located within Iowa, and all ultimately drain to the Upper Mississippi River watershed (Figure 1). Within the eight watersheds, row crop agriculture (primarily corn and soybean) was the predominant land use and ranged from 62% to 89% (Figure 1 and Table 1). Like much of the U.S. Corn Belt, the topography is quite flat. The study sites watersheds span two distinct geological regions; half of the watersheds are located in a region with karst geology, and half of the watersheds consist of poorly drained glacial till (Prior, 1991; Weary & Doctor, 2014). Hydrology in the poorly drained glacial till region has been greatly modified to speed up water removal in support of agriculture through the installation of extensive subsurface tile drainage networks (David et al., 2010).

2.2. High-Frequency Sensor Data

We used publically available high-frequency sensor data for this study collected by the U.S. Geologic Survey (USGS, http://waterdata.usgs.gov/nwis). All sensors were installed and operated by USGS who maintains an extensive network of real time sensors, including NO_3^-, throughout the Midwest where NO_3^- loads are high and relevant to downstream environmental degradation. Nitrate sensors at each site were fixed optical sensors with 2-mm path length, with the exception of the Raccoon River at Van Meter site, which has a 5-mm path length (Hach Nitratax plus sc Sensor, Loveland, CO, United States). Sensor data for nitrate was validated against traditional chemical measures of nitrate concentration by USGS personnel and following USGS protocol (Pellerin et al., 2013; Wagner et al., 2006). Nitrate sensor measurements corresponded to nitrate plus nitrite as nitrogen, denoted as NO_3^- for convenience, with an accuracy of greater than ±3% of measured value or 0.5 mg/L. Discharge, NO_3^-, and temperature sensors were colocated at each site, and

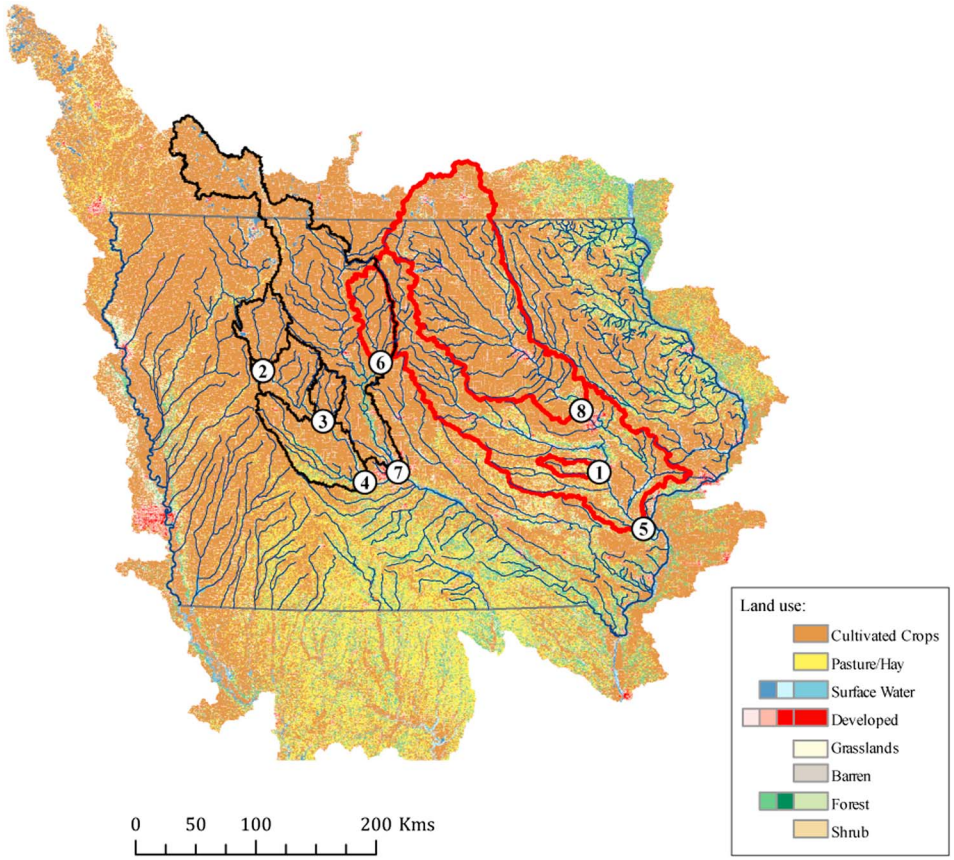

Figure 1. Gage sites and watershed characteristics. Gage sites (circles with numbers) and respective watersheds (polygons outlined in black or red) are primarily located in Iowa, United States. The predominant land use for all sites is cultivation of row crops mainly corn and soybean. Watersheds with karst geology are outlined in red. Major rivers are shown with blue lines. Land use categories are from NLCD 2011 data.

sensor data consisted of measurements collected at a 15-min interval over a period of approximately 5 years from 2012 to 2017.

All data series had gaps in the time series due to either routine maintenance or seasonality, for example, if ice had closed over the river or a sensor was removed for maintenance. The percent of gaps in each data set is provided in Table 1. Gaps in the time series had to be filled in order to perform some of the multiscale statistical analysis (described later). Gaps were filled using Auto Regressive model (fill gaps) available in Matlab R2017a with an averaging window of approximately 20 data points corresponding to 5 hr. This model is particularly effective in reconstructing large gaps in oscillating signals and, in the vicinity of the gap, gives a flexibility to select only a few samples within any segment to completely reconstruct the full signal. To test the effect of the gap-filling approach on the results, we chose 10 original time series with less than 14% missing data and introduced artificial gaps of similar size window as observed in natural data (corresponded to roughly 22% of the data) to these time series. We then refilled the gaps with the gap-filling method and compared the subsequent multiscale statistics of these to the original data sets using a paired samples *t* test using SAS-JMP software (JMP Pro 13.1.0, SAS Institute Inc., Cary, North Carolina, United States).

2.3. Multiscale Statistical Analysis

We used several statistical measures to understand and quantify across-scale nitrate dynamics and its interaction with discharge and temperature over the full five-year record for each site. These measures included power spectral density (PSD), exceedance probability, scatter plots, and cross-correlation analysis. For example, Figure 2 shows a significant variability for a range of scales for Q, NO_3^-, and T. PSD curves were used to evaluate the variability within each signal of interest, here $Q(t)$, $NO_3^-(t)$ and $T(t)$, over a range of temporal

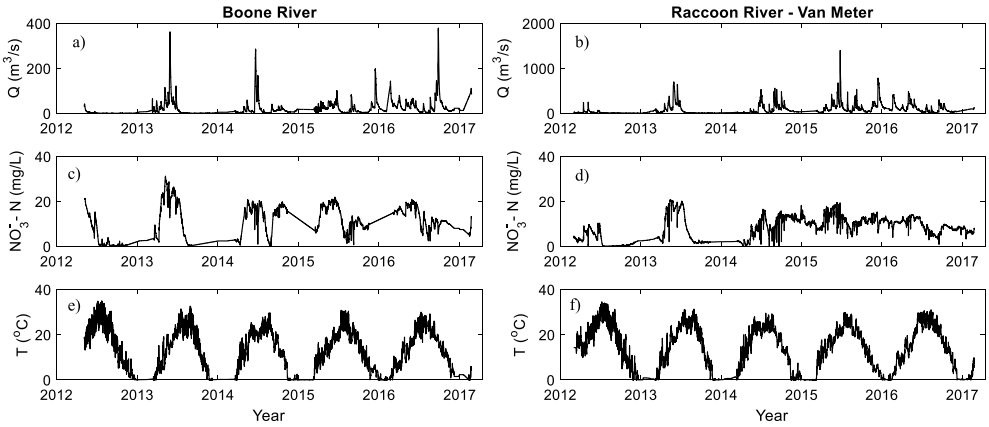

Figure 2. Filled time series of (a, b) discharge (Q), (c, d) nitrate (NO_3^-) concentration, and (e, f) water temperature (T) simultaneously collected at the sites of Boone River (left panels) and Raccoon River-Van Meter (right panels). The data were collected at a sampling interval of 15 min from 2012 to 2017.

scales and to check if the change in variability of these processes, across scales, follow certain similar characteristics or patterns. PSD of a signal $X(t)$ can be computed by finding the product of the Fourier transform of $X(t)$ and its complex conjugate (Stoica & Moses, 1997; von Storch & Zwiers, 2003). By computing the PSD, one can identify the contribution of each frequency to the time series as well as any persistent behavior that dominates within the time series. In other words, PSD can be used to detect systematic periodicities, which appear as peaks, for each evaluated variable in their corresponding time series. In addition, PSD curves exhibiting a power law regime (log-log linear behavior) across scales may suggest self-similarity and long-range dependence in the signal (Flandrin, 1989; Saupe, 1988; Singh et al., 2011). The scaling exponent of these power law regimes, that is, the slope of the PSD curve (β), characterizes change in variability with changing scales. A high value of β indicates higher long-range dependence in the signal (Saupe, 1988; Singh et al., 2011, 2012). The PSD analysis requires that the time series must be continuous and stationary over the time scales of interest. These data appear to be stationary across the duration of the time series but had seasonally occurring gaps, which were filled as is described in section 2.2. Special emphasis was placed on scaling regime that is the range of scales where PSD showed log-log linear behavior.

The behavior of the extreme fluctuations in the time series of discharge and nitrate was analyzed using exceedance probability plots. These plots characterize the probability of exceeding a certain value or event (X_j) of interest in a time series and can be related mathematically to cumulative distribution function as $P(X_j \geq x) = 1 - F(x)$, where $F(x)$ is the cumulative distribution function of a variable x and $P(X_j \geq x)$ is the probability of exceedance (e.g., Clauset et al., 2009; Singh et al., 2012). These plots can further be used to analyze (estimate) the truncation behavior (values) of a process represented by the time series. Exceedance probability was analyzed using raw, unfilled data.

Cross correlation was evaluated between all three variables analyzed here and used to assess interactions. In general, cross correlation provides a quantitative measure of linear dependence or waveform similarity between two stationary time series (Stoica & Moses, 1997). The similarity of two time series can be expressed using the cross-correlation coefficient. A cross (correlation) coefficient near zero indicates that the two time series are completely dissimilar and a value near 1 indicates high similarity. For example, a high cross correlation between nitrate concentration and discharge would indicate the importance of hydrological controls on nitrate. Similarly, the cross correlation between temperature and nitrate can be used as an indicator of biogeochemical activity. We also evaluated the correlation between discharge and water temperature, which may provide insight into water source (deep groundwater stores versus shallow subsurface or surface water). Cross-correlation analysis was, by necessity, performed using gap-filled data.

2.4. Geospatial Analysis

Geospatial characteristics for the contributing drainage area, that is, watershed, for each sampling station were determined in order to identify large-scale differences in landscape characteristics that may be

Table 2
Statistics From Time Series Analysis

		Spectral slope (β)			Cross correlation			Peak		
					CC	CC	CC	Q	NO_3	T
Site #	Site name	β_Q	β_N	β_T	Q versus NO_3	NO_3 versus T	Q versus T	(m^3/s)	(mg/L)	(°C)
1	Old Man's Creek	2.52	2.22	N/A	0.15	N/A	N/A	59.4	11.9	N/A
2	North Raccoon River-Sac City	3.14	2.52	2.90	0.31	−0.11	−0.04	138.7	22.7	28.9
3	North Raccoon River-Jefferson	3.24	2.50	2.82	0.48	0.03	0.03	267.4	26.5	29.8
4	Raccoon River-Van Meter	3.12	2.42	2.92	0.45	0.03	0.04	611.3	19.5	30.2
5	Iowa River	2.40	2.43	N/A	0.58	N/A	N/A	1656	12.8	29.8
6	Boone River	2.38	2.32	2.79	0.40	0.11	−0.03	190.9	28.6	29.8
7	Des Moines River	2.56	2.14	2.33	0.47	0.05	0.31	506.6	17.2	28.8
8	Cedar River	2.36	2.29	2.60	0.39	−0.04	0.12	1500	15.1	28.1

Note. Peak values (last three columns) correspond to 99th percentile values for all measurements, that is, with $<$ 1% exceedance probability during the period of analysis. N/A = not applicable.

controlling multiscale behavior of the time series. In this study we quantified contributing drainage area size, land use, and karst geology for each monitoring station using spatial data in ArcGIS (ESRI ArcGIS Desktop release 10.3.1, Redlands, CA, 2015). Contributing drainage area was delineated using topography from a 30-m digital elevation model and watershed delineation tools available within ArcGIS. Land use was classified with the National Land Cover Database 2011 (NLCD 2011) as described in Homer et al. (2015). NLCD 2011 land use data were visually compared to crop data from the U.S. Department of Agriculture National Agriculture Statistics Services data layer (U.S. Department of Agriculture, 2014) to verify that there was no significant change over the period of our study. Karst geology was classified with a USGS open source data layer (Weary & Doctor, 2014). Watershed land use and geological characteristics for each site were determined by intersecting the appropriate data layer with the contributing drainage area using the intersect tool within ArcGIS. Relationships between the statistical measures of multiscale behavior and watershed characteristic metrics were evaluated using linear regression analysis and quantified using the Statistics Toolbox in Matlab R2015b.

3. Results

All analyses were performed for all sites; however, for brevity, we have chosen selective sites to illustrate general behavior. These sites include Boone River, Des Moines River, Old Man's Creek, and North Raccoon River at Sac City. These sites span a range in crop cover, watershed area, and karst conditions and illustrate all of the observed responses. Results metrics for all sites are provided in Table 2 and relevant plots for the remaining sites are provided in supporting information (Figure S1).

3.1. Multiscale Temporal Behavior

Figure 2 shows the gap-filled time series plots for discharge, NO_3^-, and temperature for Boone River watershed (Figure 2, left panels) and Raccoon River-Van Meter watershed (Figure 2, right panels). A clear annual periodic behavior can be observed in the temperature time series. In addition, larger peaks in the discharge can be seen correlating with larger peaks in NO_3^-. The discharge and NO_3^- show differing patterns when compared for the same time across the two sites (for example, comparing 2016 data), whereas the temperature time series show very similar patterns (e.g., same magnitude annual periodicity) for these sites suggesting different variability patterns in the three considered time series.

In the frequency domain, power law behavior was evident across a range of temporal scales for Q, NO_3^-, and T for all sites (Figure 3 and Table 2). For example, Figure 3 shows the PSD for Q and NO_3^- for Old Man's Creek (Figures 3a and 3d), Des Moines River (Figures 3b and 3e), and North Raccoon River at Sac City (Figures 3c and 3f). These three sites represent examples of responses from watersheds with low (Old Man's Creek), medium (Des Moines River), and high (North Raccoon River at Sac City) percentage crop cover. The scaling exponent, that is, the slope of the log-log region of the PSD curve (β) for all three variables were very similar and lie within [2.14 to 3.24] (Table 2). All values were greater than two indicating positive autocorrelation, that is, persistent behavior across scales (Singh et al., 2012). Nitrate PSDs show single-scaling regime for

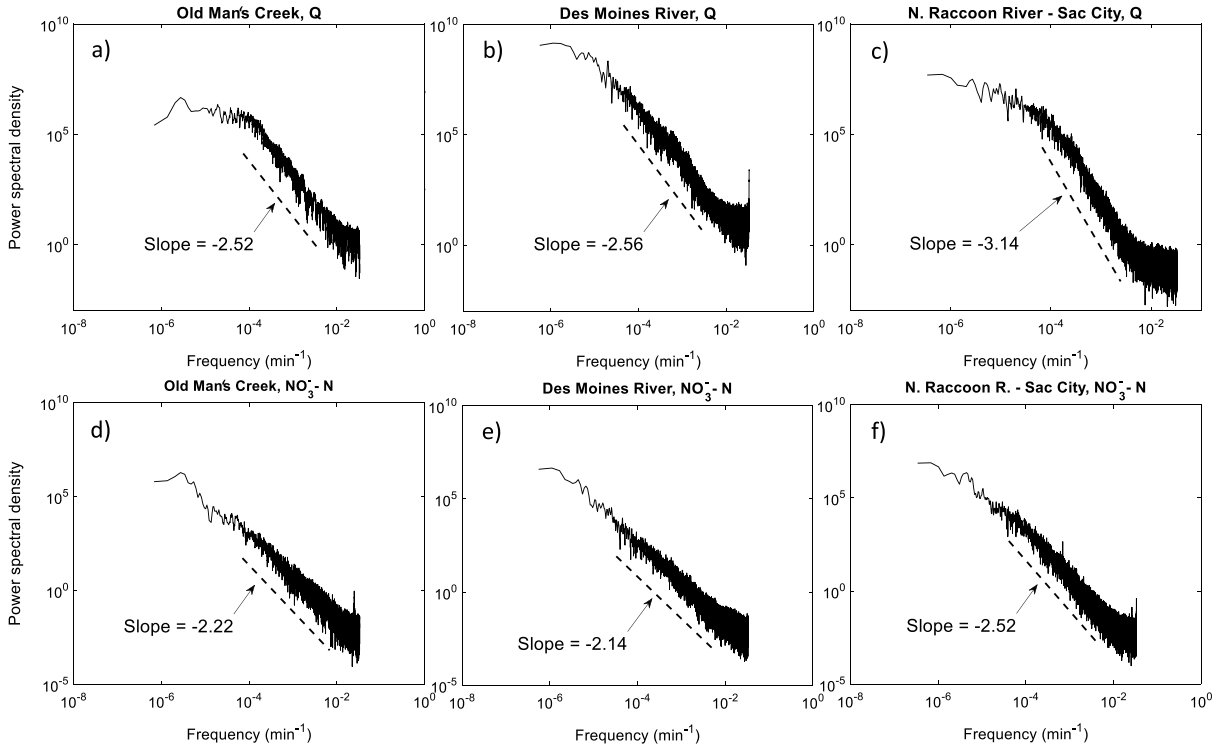

Figure 3. Power spectral density of (a–c) discharge (Q) and (d–f) nitrate (NO_3^-) at three sites corresponding to different cropland coverage, that is, with low (Old Man's Creek), medium (Des Moines River), and high (North Raccoon River-Sac City) percentage crop cover.

all the analyzed sites, whereas a scaling regime appears to break (i.e., change slope) in the PSD of discharge. Note that the scaling range for which βs were computed was the same for Q, NO_3^-, and T (range of 100 min to 7 days). The suggestive slopes (β) of the linear range of the PSDs (shown as dashed lines on the side in Figure 3 and summarized in Table 2) were always higher for T than for NO_3^- within a site (Table 2) indicating lower-frequency responses in temperature data than nitrate data for a given site. There was no apparent trend across β_Q and β_N or β_T, where β_Q and β_N or β_T represent slope of scaling regime for the PSDs of discharge, NO_3^-, and temperature, respectively.

Strong peaks in the PSD curve were observed at frequencies corresponding to the annual scale ($2 \cdot 10^{-6}$ min^{-1}) for all sites for temperature (Figures 4a and 4e). Additional peaks were seen in the PSD for water temperature at frequencies corresponding to diurnal periodicity ($7 \cdot 10^{-4}$ min^{-1}). Diurnal periodicity was not detected for NO_3^- or discharge with this analysis, although could be observed in late summer in subsections of the time series for some sites (Figures 4d and 4e).

Gaps in the time series occurred primarily in the winter season and appear to follow a seasonal pattern. Mean and standard deviation of the percent of missing data for Q, NO_3^-, and T were 13.6 ± 7.54%, 26 ± 10.84%, and 9.08 ± 7.13%, respectively. We tested the effect of gap filling on our results by creating artificial gaps in 10 time series and comparing results from the gap-filled and original time series. Based on a paired samples t test of PSD slope between the two groups, there was no significant difference between the original time series and the gap-filled time series ($t(18) = 0.057$, $p = 0.96$). Percent error introduced by gap filling for individual sites was, on average, less than 2% (maximum = 4.9%, minimum = 0.14%). Statistical test results suggest that the gap-filling approach is robust, at least for the seasonal gaps, which were present in this data set. The sensitivity of results to changing PSD window size was also tested and was confirmed to not appreciably change the results for window sizes up to 150 data points.

Figure 5 shows log-log plots for the probability of exceedance, which quantifies the probability of exceeding a certain magnitude of event, for NO_3^- (Figure 5a) and discharge (Figure 5d). Peak values were defined as the concentration corresponding to 99th percentile or exceeded less than 1% of time. When normalized with peak Q, watersheds showed similar behavior across a range of scales except for Des Moines River and Old

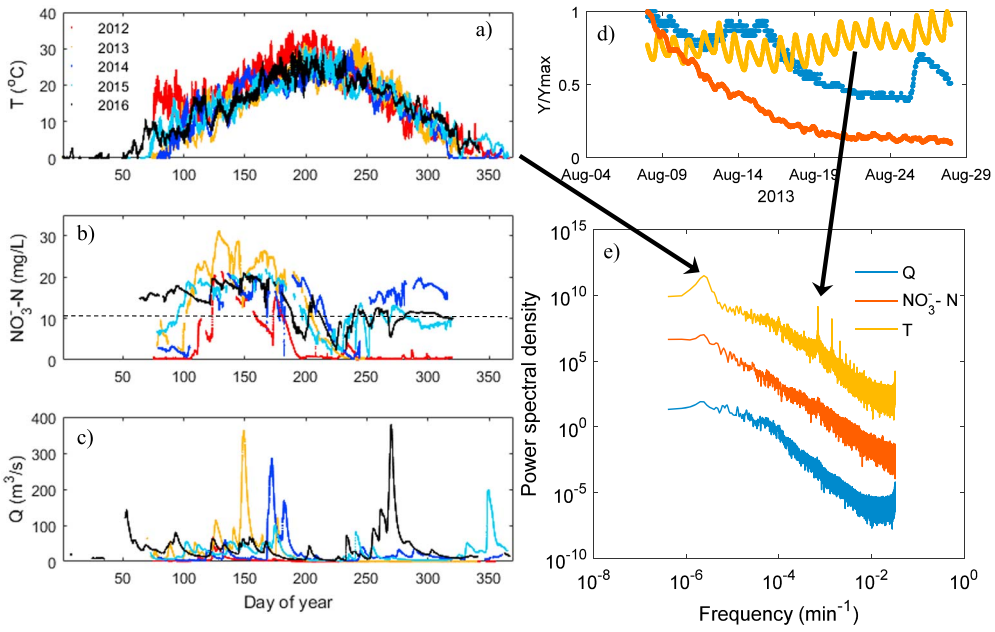

Figure 4. Periodicities in three analyzed variables, that is, temperature (a), nitrate (b), and discharge (c) obtained from Boone River watershed. Dashed line in (b) is USEPA United States Environmental Protection Agency drinking water consumption limit (10 mg/L). Note that these figure panels show data for five different years to compare similarities in periodicity. Panel (d) shows zoomed-in time series for approximately 3 weeks for the year 2013. (e) Power spectral density of discharge, nitrate concentration, and water temperature. Orange, red, and blue colors in (d) and (e) correspond to temperature, nitrate, and discharge, respectively, whereas the two arrows point toward distinct annual and diurnal periodicity in temperature power spectral density. Frequencies greater than 3.5×10^{-2} were attributed to noise and were removed for display purposes. The *y* axis in (e) represents arbitrary scales.

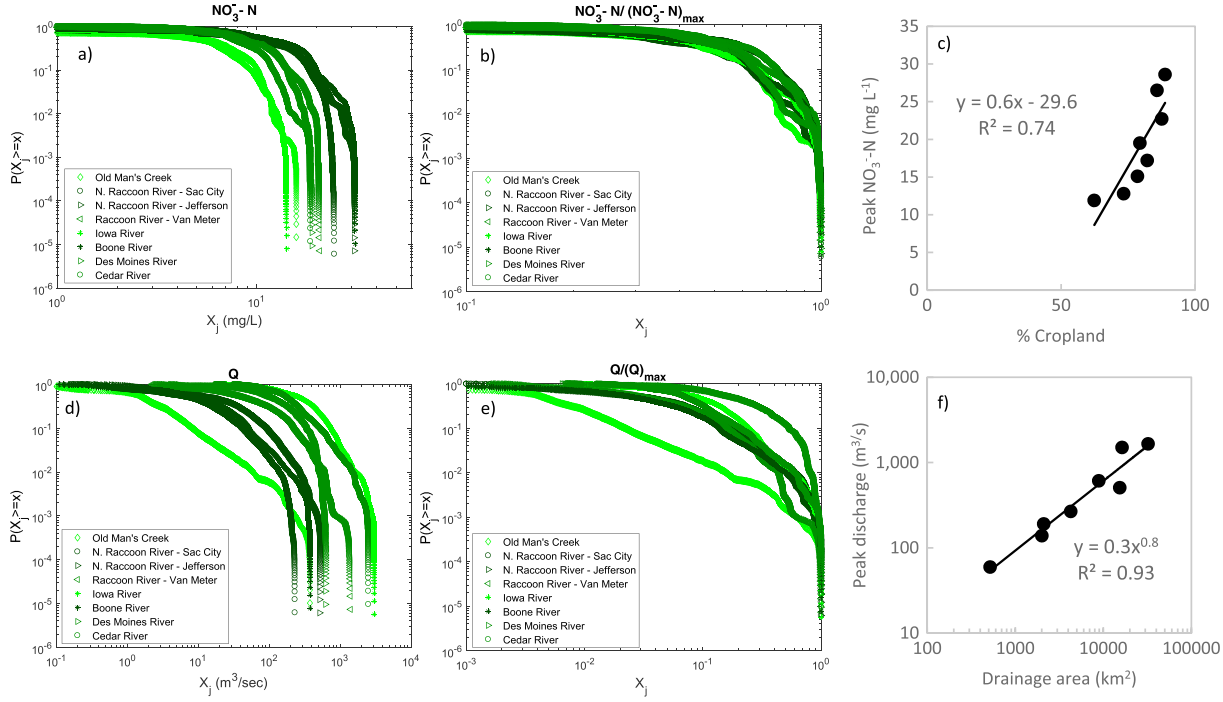

Figure 5. Exceedance probability characteristics for nitrate concentration (a–c) and discharge (d–f). Marker shape denotes site and marker color denotes fraction of contributing area used for row crop agriculture (Table 1). Panels (b) and (e) show normalized (divided by maximum value) nitrate and discharge, respectively. Peak nitrate increased significantly with increases in crop cover ($p = 0.006$), and peak discharge increased significantly with increases in drainage area ($p < 0.0001$).

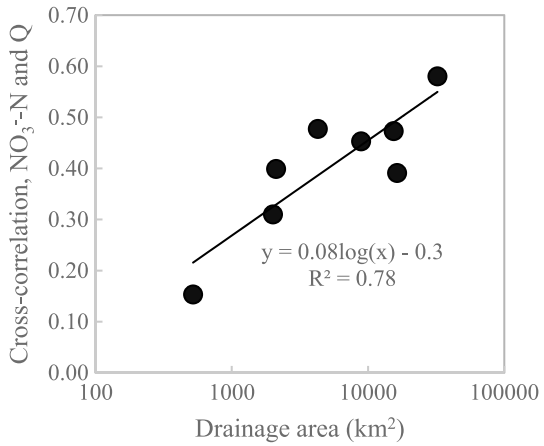

Figure 6. Cross-correlation between discharge and nitrate concentration. A log linear behavior of cross correlation is observed with increasing contributing drainage area.

Man's Creek (Figure 5e). For the case of NO_3^-, all normalized exceedance probability plots displayed similar curvature (Figure 5b).

Cross correlation was evaluated between NO_3^-, Q, and T to determine the degree of similarity in the variances of the time series. For all sites cross correlation was greatest between Q and NO_3^- as compared to Q with T or NO_3^- with T. Cross correlation was near zero for NO_3^- and T and for Q and T (Table 2). The one exception to this was a positive cross correlation between Q and T at the Des Moines River site, which is located immediately downstream of a reservoir (Table 2).

3.2. Watershed Characteristics

Spatial characteristics of the watersheds was evaluated including drainage area, extent of karst geology, and land use (Table 1). Drainage areas for the eight sites ranged from a minimum of 521 km^2 at Old Man's Creek to a maximum of 32,375 km^2 at Iowa River. The extent of karst geology underlying each watershed was reported as above or below 50% areal extent throughout the watershed. Out of eight study sites, four sites had less than 50% karst geology and four sites had greater that 50% karst geology. Sites with karst geology were grouped together and located on the eastern side of the state of Iowa, whereas sites with low karst geology were on the western or central part of the state. The primary land use for all watersheds was row crop agriculture. The average extent of crop cover across all sites was 80% with the highest crop cover in the Boone River watershed (89%) and the lowest crop cover in the watershed for Old Man's Creek (62%). Wetland cover, developed land use, and forested cover did not vary much across watersheds (Table 1). Grassland and cropland were linearly, inversely proportional ($R^2 = 0.94$) with grassland cover at a minimum for Boone River (2.5%) and a maximum for Old Man's Creek (26.2%).

3.3. Multiscale Temporal Dynamics and Watershed Characteristics

The distributions in PSD curve slopes for discharge (β_Q) for sites with karst and nonkarst geology differed significantly (Mann-Whitney test, $n_1 = n_2 = 4$, $p = 0.03$). Mean values, with standard deviation in parentheses, for β_Q for karst and nonkarst sites were 2.45 (0.09) and 2.99 (0.29), respectively. In contrast to β_Q, we did not see a difference in the distributions of β_N between karst and nonkarst geology (Mann-Whitney test, $n_1 = n_2 = 4$, $p = 0.83$). Mean values for β_N for karst and nonkarst sites were 2.37 (0.15) and 2.40 (0.18), respectively. At sites with karst geology, peaks in the PSD curve were also observed at frequencies corresponding to the annual scale for NO_3^- and discharge (Figures 3 and S1).

Across all eight sites, the cross correlation of Q with NO_3^- was significantly related to the log drainage area and increased with drainage area (Figure 6, $n = 8$, $R^2 = 0.78$, $p = 0.004$). Note that correlation does not necessarily imply causality, and if two data series are strongly autocorrelated, it is possible to get spurious correlations (Cryer & Chan, 2008). As can be seen from Figure 5d, Q show significant variability in exceedance probability curves for the sites analyzed here due to varying watershed drainage area. Peak Q was significantly related to drainage area by $Q_{peak} = 0.33\ (\text{watershed area})^{0.82}$ (Figure 5f, $R^2 = 0.93$, $n = 8$, $p < 0.0001$).

NO_3^- exceedance probability shows striking similarities when grouped based on crop cover (Figure 5a) and was significantly related to crop cover by $y = 0.61x - 30$, where y is peak NO_3^- and x is cropland fraction of the watershed (Figure 5c, $r^2 = 0.74$, $n = 8$, $p = 0.006$).

3.4. Event Responses

Large changes in NO_3^- tended to co-occur with large changes in Q as can be seen in the time series data (Figure 2b). In general, changes in NO_3^- were rapid on the rising limb of the event hydrograph and could be either positive (concentrating) or negative (diluting), whereas on the falling limb of the hydrograph, NO_3^- and Q were decoupled and NO_3^- was rising or stable, regardless of whether the initial response to discharge had been a positive or negative change. At peak Q, NO_3^- was either low, presumably due to overland flow, or was continuing to rise. Further, after an event, NO_3^- typically remained elevated much longer that Q. These opposing responses are illustrated in Figure 7 with data from North Raccoon River-Jefferson during April and May 2015. Note the three concentrating event responses which occurred in April and early May

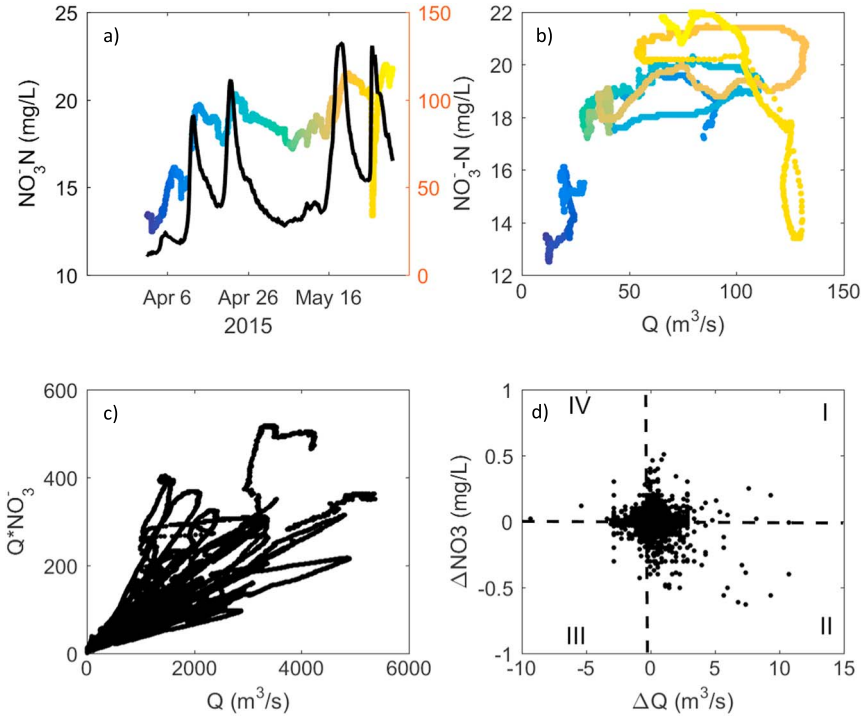

Figure 7. (a) Subsection of time series of nitrate in colors (represented by left *y* axis) and discharge in black (represented by right *y* axis) for the 2 months (April and May of year 2015) at North Raccoon River at Jefferson depicting event-scale response of NO_3^- to discharge, which can be either concentrating or diluting depending in part on nitrate concentration prior to the event, and lag between event and event magnitude. (b) NO_3^--*Q* trajectories for the same period of time as shown in panel (a) demonstrate hysteresis in the NO_3^- in response to *Q*. Analysis across the entire record show that the highest nitrate loads can occur at intermediate discharge (c) and that the variation in NO_3^- responses to changing discharge is greatest for the rising limb of an event hydrograph (d).

versus one diluting event response seen in the last event in May (Figure 7a). This dichotomy in responses can be seen on a NO_3^--*Q* bi-plot, which illustrates the hysteresis in the relationship through the various trajectories (Figure 7b). Note that the maximum spring NO_3^- concentration occurred at intermediate *Q* (Figure 7b) as does the maximum overall nitrate load (Figure 7c).

We considered the direction and magnitude of change in *Q* and NO_3^- in Figure 7d for all available data from North Raccoon River-Jefferson. These data can be categorized by the four potential quadrants they fall within. Quadrants I and II correspond to positive changes in *Q*, that is, the rising limb, and quadrants III and IV correspond to negative changes in *Q*, that is, the falling limb. Similarly, quadrants I and IV correspond to positive changes in NO_3^-, that is, concentration, whereas quadrants II and III correspond to negative changes in NO_3^-, that is, dilution. We found that the distribution of data was almost identical between these quadrants (25.4%, 24.5%, 25.2%, and 24.9%); however, the variance was much higher in quadrant II than in the other three (0.68 in quadrant II, compared to 0.58, 0.44, and 0.37 in quadrants I, III, and IV, respectively; see Figure 7d).

4. Discussion

Our results support our first hypothesis, that is, that the relative importance of hydrological and biogeochemical processes toward NO_3^- export can be extracted from multiscale temporal NO_3^-, *Q*, and *T* statistics. We observed patterns in PSD slopes and spikes, cross correlation between variables, and relative magnitudes in exceedance probability curves across sites that all provided information that was used to interpret the processes controlling nitrate dynamics. Our results do not fully support our second hypothesis, that is, that the magnitude of NO_3^- export under extreme discharge conditions can be determined through analysis of NO_3^- and *Q* time series data. Although each watershed did asymptotically approach peak NO_3^- and peak *Q* values,

NO_3^- and *Q* were decoupled in time and peak NO_3^- export often occurred at intermediate *Q*. The implications of these results along with the limitations and opportunities of the analytical method are further discussed below.

4.1. Hydrological and Biogeochemical Process Controls on NO_3^-

Multiscale analysis of environmental sensor time series data can reveal underlying across-scale behaviors that provide additional insight into the processes controlling the signal behavior. We show that hydrology and terrestrial biogeochemical processes are the primary controls on NO_3^- dynamics at the eight sites we studied. We observed cross-correlation between NO_3^- and *Q* for all sites, which increased log-linearly with drainage area (Figure 6 and Table 2). This suggests that hydrology or terrestrial biogeochemical processes, both which scale with area, are the primary controls on nitrate dynamics. We also saw that the magnitude of the exceedance probability curve increased with crop cover, suggesting terrestrial nitrogen inputs are important at all time scales.

In contrast, there is little evidence of in-channel biogeochemical influence on NO_3^- when considered across scales. We did not observe cross-correlation between NO_3^- and *T* (Table 2). Furthermore, although we see evidence of diurnal NO_3^- cycling in the time series from late summer, low flow conditions (Figure 4d), it is either not persistent enough across the entire time series or too weak compared to other processes to be regulating the signal. Neither is there a corresponding distinct diurnal peak in the NO_3^- PSD although there is in the temperature PSD (Figure 3). Together these observations indicate that in-channel biogeochemical processes, which remove or transform nitrogen, are either overwhelmed by the role of hydrology or that their interaction with nitrate does not transcend temporal scales within the intensively managed agricultural watersheds in this study.

Discharge, NO_3^-, and temperature all exhibited log-log linear scaling regimes in PSD across all watersheds and over a range of scales suggesting power law behavior for all sites (Figure 3). To the best of our knowledge, power law behavior in the PSD of NO_3^- has not been reported before for intensively agriculturally managed watersheds although has been considered in watersheds with mixed land use (Aubert et al., 2014; Rode et al., 2016) and has been observed for discharge in several studies in the past (e.g., Keylock, 2012; Sandhu et al., 2016). The slope in the PSD of nitrate (on average ~2.4) suggests a persistent behavior of nitrate across spatial and temporal scales. This slope is much higher than that observed by Rode et al. (2016) who report β_N near 1. All β_N in our study were greater than 2, indicating that nitrate response dynamics in the region are highly persistent (Basu et al., 2010).

Connections between the statistics describing multiscale temporal behavior and the statistics describing geospatial characteristics of the landscape confirmed our conclusions about the role of hydrological and biogeochemical controls on NO_3^- dynamics within the study basins. The influence of land use patterns and NO_3^- inputs was clearly seen in the NO_3^- time series data. Crop cover was predictive of the relative magnitude of NO_3^- for all probabilities of exceedance from the eight sites (Figure 5a) and, notably, of peak NO_3^- from the eight sites (Figure 5c). A positive relationship between crop cover and NO_3^- has previously been reported for the Corn Belt (Blesh & Drinkwater, 2013; Hansen et al., 2018; Howarth et al., 2012; Sobota et al., 2013) and, together with the results of this study, indicate that the primary source of riverine NO_3^- in this region is agriculture. It is not known whether this relationship is due to current or historical patterns of agricultural nitrogen inputs.

Geology was found to effect the multiscale dynamics of *Q* but not NO_3^- indicating that little biogeochemical transformation of nitrogen is occurring within karst storage zones. PSD slopes for discharge (β_Q) differed significantly for sites with karst and nonkarst geology with lower β_Q observed for karst sites. Lower β values indicate lesser persistence (memory) within a process that is consistent with scientific understanding of karst geology being characterized by a wide range in travel time (Mellander et al., 2013). Nonkarst sites in this study likely had subsurface tile drainage, which is also a rapid subsurface water conduit although a larger volume of water is typically stored in karst between events. In contrast to β_Q, we did not see a difference in the distributions of β_N between karst and nonkarst geology whose means were nearly identical despite the capacity of karst to decouple surface water chemistry from land use (Schilling & Helmers, 2008). Since little water would be stored in subsurface tile drainage, the lack of difference in β_N between karst and nonkarst sites indicates that the influence of biogeochemical processes within karst on surface water NO_3^- were minimal.

4.2. Nitrate Response to Extreme Discharge Events

The second hypothesis of this study was that multiscale temporal dynamics could be used to predict NO_3^- response to extreme climatic events. This hypothesis was not strictly supported due to limitations of the method. Although information gained from the analysis informs which sites might be most vulnerable to increasing precipitation frequency or magnitude, further information about temporal lags between NO_3^- and *Q* are needed to predict changes in export.

The results of this study can provide insight into which landscape characteristics are most likely to result in a larger response in nitrate load to predicted changes in climate. The nitrate load for a landscape is a function of the shape of the temporal response of *Q* and NO_3^-, the offset between the peaks in *Q* and NO_3^-, and the magnitude of the peaks. Multiscale analysis provided insight into the likely magnitude of the peaks, and, as was seen in our results, peak NO_3^- increased significantly with increases in crop cover and peak *Q* with drainage area. Multiscale analysis alone provides enough information to evaluate the worst-case loading scenario under the assumption that NO_3^- and *Q* are aligned and responses in time are rapid and is useful in order to put an upper bound on climate risk. However, additional information contained in the shape of the time series response curves is required to fully predict NO_3^- export.

Cross-correlation coefficients indicated that *Q* and NO_3^- were highly correlated (Figure 6); however, *Q* versus NO_3^- bi-plots and overlaid time series reveal the presence of time lags, that is, hysteresis in NO_3^- response (Figure 7). This temporal offset results in the highest NO_3^- concentrations and loads often occurring at intermediate *Q* and not peak *Q* (Figures 7b and 7c) as previously reported for the region (Jones et al., 2017). Hysteresis in the response of NO_3^- to *Q*, has been previously reported in landscapes with more heterogeneous land use (Blaen et al., 2017; Carey et al., 2014; Lloyd et al., 2016). The hysteresis response we report on an event scale is consistent with recent studies indicating that annual patterns in nitrate loads vary in response to wet vesus dry conditions during the previous year (Davis et al., 2014; Loecke et al., 2017) although could be, in part, due to variability in precipitation intensity or distribution between events (Pellerin et al., 2014).

The temporal offset, that is, hysteresis, likely indicates that precipitation events are initiating or accelerating terrestrial nitrogen transformation processes that increase the supply of NO_3^-, that is, mineralization then nitrification, which likely occurs at slower time scales than event runoff for the analyzed landscape. These biogeochemical processes are transforming the available nitrogen on time scales longer than the event scale but shorter than the interevent scale and are potentially triggered by hydrology. If the temporal lag was due to hydrological connections or disconnections from water sources with different NO_3^-, then the bi-plot would be a single curved line, which would be horizontal if the landscape was chemostatic with respect to NO_3^-, that is, not responsive to discharge. Landscapes with sharper changes in the curvature of the NO_3^- time series response curve, for example, if the mineralization to nitrification process was relatively fast, would result in greater increases in nitrate load by increasing NO_3^- on the falling limb of the hydrograph. Watersheds where stored nitrogen was already in the form of NO_3^-, for example, in groundwater as opposed to soil organic matter, would presumably have less lag between peak NO_3^- and peak *Q* although the effect of such a system on hydrology is not known. A more slowly changing hydrograph, such as that expected for a landscape with significant water storage or river network branching, would result in an increased *Q* at higher NO_3^-, as the movement of water is slowed down, although this could be offset by an overall decreased NO_3^- due to increased water residence time and in-stream NO_3^- removal (Czuba et al., 2018).

The offset in peak NO_3^- and peak *Q* for individual events has important implications for what precipitation patterns will have the greatest effect on NO_3^- export. Because of the offset in peak NO_3^- and peak *Q* and under current NO_3^- availability, storm frequency, not magnitude, will be the more important driver of total nitrate export. For the Midwestern United States precipitation has been predicted to increase in both frequency and magnitude (Pryor et al., 2013; Sinha et al., 2017). If precipitation event frequency increases, then multiple events in close succession could greatly increase nitrate loads by increasing the transport of NO_3^- that was mobilized by the first event as well as releasing additional nitrogen stores into the soluble form of NO_3^-. In contrast, higher magnitude but lower frequency events would increase nitrate export during a single event, due to greater time between events for nitrogen to accumulate in the soils, as has been noted previously (Loecke et al., 2017). Finally, events which occur shortly after fertilizer application, would also amplify the output due to larger sources of nitrogen on the landscape.

4.3. Limitations of Method

Multiscale time series analytical methods have been widely applied in hydrology and other disciplines. Our study illustrates that these methods could contribute toward greater understanding of persistent process controls on water quality indicators, such as nitrate, especially as high-frequency sensor data becomes more widely available. However, there are several limitations to the method that must be considered including; the assumption of signal stationarity, requirement for signal continuity, and loss of information about the data sequence.

One of the primary assumptions of some forms of frequency analysis, such as spectral analysis and cross-correlation analysis, is that the time series is at least weakly stationary. This requirement limits the length of environmental time series which could be subject to this form of analysis to lengths long enough to span multiple known seasonal patterns but short enough to avoid longer term responses to changes in climate or land use. Second, some multiscale statistical methods require evenly spaced, continuous data series. This is not always possible for environmental sensors where, factors such as extreme high or low discharge, seasonal changes in temperature, or biofouling may necessitate the temporary removal of sensors from the environment. For example, in temperate regions such as our sites, seasonal ice formation often precludes continuous sensor deployment. Depending on the nature of the data gap (e.g., due to maintenance versus seasonality) information about specific time scales could be absent and the subsequently required gap filling may affect the results. Although we did not see a statistically significant difference in results from the gap-filled data as tested in this study, no information was available to characterize small-scale fluctuations during winter at these sites due to the gaps. Finally, PSD is useful for pulling out dominant controls on the overall signal but may not offer much understanding to processes that are only temporarily or secondarily important, such as aquatic nitrate uptake in our study, and therefore may miss second order processes that could be amplified through appropriate system management.

5. Conclusions

Excess nitrate in streams and rivers of Midwestern United States has caused local and downstream water quality impairments extending from Upper Mississippi watersheds all the way to the Northern Gulf of Mexico. Using multiscale statistics of simultaneously sampled high-resolution discharge, nitrate, and temperature data from eight intensively managed agricultural watersheds in Iowa, United States, we evaluated how nitrate concentration (NO_3^-) interacts with discharge (Q) and water temperature (T) within these watersheds. These results suggest that, in an intensively managed agricultural landscape where NO_3^- is quite high, hydrology and terrestrial biogeochemistry overshadow the role of stream biogeochemistry in mediating nitrate dynamics. Responses to watershed geology and drainage area were also seen in NO_3^- and Q across scales. There was also evidence that terrestrial biogeochemistry moderates NO_3^-, most notably in the relationships between multiscale parameters and watershed characteristics and in persistent patterns in the time series themselves. Despite similar multiscale patterns between NO_3^- and Q and strong cross correlation between NO_3^- and Q for all watersheds, peaks in NO_3^- and Q were not temporally aligned and the highest NO_3^- often occurred at intermediate-sized discharge events. Based on this analysis, landscapes with high peak NO_3^- or less lag between peak NO_3^- and peak Q are likely to have the largest increases in NO_3^- loads in response to projected regional changes in climate.

Acknowledgments
This research was funded by the National Science Foundation (NSF) through a NSF Science, Engineering and Education for Sustainability (SEES) Fellows grant (EAR-1415206) to A. T. H. The American Geophysical Union (AGU)-Chapman Conference on Freshwater Biogeochemistry under Extreme Climatic Events was instrumental in motivating this research. A. S acknowledges partial support from the Donor of American Chemical Society Petroleum Research Fund. All raw data used for this study are publically available and can be accessed at https://waterwatch.usgs.gov/wqwatch. Gap-filled data have been deposited in a public and permanent depository and can be accessed at Singh and Hansen (2018, https://doi.org/10.13020/D6T106).

References

Aubert, A. H., Kirchner, J. W., Gascuel-Odoux, C., Faucheux, M., Gruau, G., & Mérot, P. (2014). Fractal water quality fluctuations spanning the periodic table in an intensively farmed watershed. *Environmental Science and Technology*, *48*(2), 930–937. https://doi.org/10.1021/es403723r

Aubert, A. H., Thrun, M. C., Breuer, L., & Ultsch, A. (2016). Knowledge discovery from high-frequency stream nitrate concentrations: Hydrology and biology contributions. *Scientific Reports*, *6*(1), 31536. https://doi.org/10.1038/srep31536

Basu, N. B., Destouni, G., Jawitz, J. W., Thompson, S. E., Loukinova, N. V., Darracq, A., et al. (2010). Nutrient loads exported from managed catchments reveal emergent biogeochemical stationarity. *Geophysical Research Letters*, *37*, L23404. https://doi.org/10.1029/2010GL045168

Blaen, P. J., Khamis, K., Lloyd, C., Comer-Warner, S., Ciocca, F., Thomas, R. M., et al. (2017). High-frequency monitoring of catchment nutrient exports reveals highly variable storm event responses and dynamic source zone activation. *Journal of Geophysical Research: Biogeosciences*, *122*, 2265–2281. https://doi.org/10.1002/2017JG003904

Blann, K. L., Anderson, J. L., Sands, G. R., & Vondracek, B. (2009). Effects of agricultural drainage on aquatic ecosystems: A review. *Critical Reviews in Environmental Science and Technology*, *39*(11), 909–1001. https://doi.org/10.1080/10643380801977966

Blesh, J., & Drinkwater, L. E. (2013). The impact of nitrogen source and crop rotation on nitrogen mass balances in the Mississippi River Basin. *Ecological Applications*, *23*(5), 1017–1035. https://doi.org/10.1890/12-0132.1

Carey, R. O., Wollheim, W. M., Mulukutla, G. K., & Mineau, M. M. (2014). Characterizing storm-event nitrate fluxes in a fifth order suburbanizing watershed using in situ sensors. *Environmental Science and Technology*, *48*(14), 7756–7765. https://doi.org/10.1021/es500252j

Clauset, A., Shalizi, C. R., & Newman, M. E. J. (2009). Power-law distributions in empirical data. *SIAM Review*, *51*(4), 661–703. https://doi.org/10.1137/070710111

Cryer, J. D., & Chan, K. S. (2008). *Time series analysis with applications in R* (2nd ed.). New York: Springer Science+Business Media, LLC.

Czuba, J. A., Hansen, A. T., Foufoula-Georgiou, E., & Finlay, J. C. (2018). Contextualizing wetlands within a river network to assess nitrate removal and inform watershed management. *Water Resources Research*, *54*, 1312–1337. https://doi.org/10.1002/2017WR021859

David, M. B., Drinkwater, L. E., & Mclsaac, G. F. (2010). Sources of nitrate yields in the Mississippi River Basin. *Journal of Environmental Quality*, *39*(5), 1657–1667. https://doi.org/10.2134/jeq2010.0115

Davis, C. A., Ward, A. S., Burgin, A. J., Loecke, T. D., Riveros-Iregui, D. A., Schnoebelen, D. J., et al. (2014). Antecedent moisture controls on stream nitrate flux in an agricultural watershed. *Journal of Environmental Quality*, *43*(4), 1494. https://doi.org/10.2134/jeq2013.11.0438

Diaz, R. J., & Rosenberg, R. (2008). Spreading dead zones and consequences for marine ecosystems. *Science*, *321*(5891), 926–929. https://doi.org/10.1126/science.1156401

Downing, B. D., Bergamschi, B. A., & Kraus, T. E. C. (2017). Synthesis of data from high-frequency nutrient and associated biogeochemical monitoring for the Sacramento–San Joaquin Delta, northern California, U.S. Geological Survey Scientific Investigations Report 2017 – 5066.

Dubrovsky, N. M., Burow, K.R., Clark, G.M., Gronberg, J.M., Hamilton P.A., Hitt, K.J., et al. (2010). The quality of our nations water—Nutrients in the nation's streams and groundwater, 1992-2004, U.S. Geological Survey Circular 1350. Retrieved from http://water.usgs.gov/nawqa/nutrients/pubs/circ1350, (Accessed on November 20, 2012).

Flandrin, P. (1989). On the spectrum of fractional Brownian motions. *IEEE Transactions on Information Theory*, *35*(1), 197–199. https://doi.org/10.1109/18.42195

Galloway, J. N., Dentener, F. J., Capone, D. G., Boyer, E. W., Howarth, R. W., Seitzinger, S. P., et al. (2004). Nitrogen cycles: Past, present, and future. *Biogeochemistry*, *70*, 153–226.

Goolsby, D. A., Battaglin, W. A., Aulenbach, B. T., & Hooper, R. P. (2000). Nitrogen flux and sources in the Mississippi River Basin. *The Science of the Total Environment*, *248*(2–3), 75–86. https://doi.org/10.1016/S0048-9697(99)00532-X

Hansen, A. T., Dolph, C. L., Foufoula-Georgiou, E., & Finlay, J. C. (2018). Contribution of wetlands to nitrate removal at the watershed scale. *Nature Geoscience*, *11*(2), 127–132. https://doi.org/10.1038/s41561-017-0056-6

Helton, A. M., Hall, R. O., & Bertuzzo, E. (2017). How network structure can affect nitrogen removal by streams. *Freshwater Biology*, 1–13. https://doi.org/10.1111/fwb.12990

Homer, C. G., Dewitz, J. A., Yang, L., Jin, S., Danielson, P., Xian, G., et al. (2015). Completion of the 2011 National land cover database for the conterminous United States—Representing a decade of land cover change information. *Photogrammetric Engineering and Remote Sensing*, *81*(5), 345–354.

Howarth, R., Swaney, D., Billen, G., Garnier, J., Hong, B., Humborg, C., et al. (2012). Nitrogen fluxes from the landscape are controlled by net anthropogenic nitrogen inputs and by climate. *Frontiers in Ecology and the Environment*, *10*(1), 37–43. https://doi.org/10.1890/100178

Howarth, R. W., & Marino, R. (2006). Nitrogen as the limiting nutrient for eutrophication in coastal marine ecosystems: Evolving views over three decades. *Limnology and Oceanography*, *51*(1part2), 364–376. https://doi.org/10.4319/lo.2006.51.1_part_2.0364

Jones, C. S., Wang, B., Schilling, K. E., & Chan, K. (2017). Nitrate transport and supply limitations quantified using high-frequency stream monitoring and turning point analysis. *Journal of Hydrology*, *549*, 581–591. https://doi.org/10.1016/j.jhydrol.2017.04.041

Keylock, C. J. (2012). A resampling method for generating synthetic hydrological time series with preservation of cross-correlative structure and higher-order properties. *Water Resources Research*, *48*, W12521. https://doi.org/10.1029/2012WR011923

Lark, T. J., Meghan Salmon, J., & Gibbs, H. K. (2015). Cropland expansion outpaces agricultural and biofuel policies in the United States. *Environmental Research Letters*, *10*(4), 44003. https://doi.org/10.1088/1748-9326/10/4/044003

Lloyd, C. E. M., Freer, J. E., Johnes, P. J., & Collins, A. L. (2016). Using hysteresis analysis of high-resolution water quality monitoring data, including uncertainty, to infer controls on nutrient and sediment transfer in catchments. *Science of the Total Environment*, *543*(Pt A), 388–404. https://doi.org/10.1016/j.scitotenv.2015.11.028

Loecke, T. D., Burgin, A. J., Riveros-Iregui, D. A., Ward, A. S., Thomas, S. A., Davis, C. A., & Clair, M. A. S. (2017). Weather whiplash in agricultural regions drives deterioration of water quality. *Biogeochemistry*, *133*(1), 7–15. https://doi.org/10.1007/s10533-017-0315-z

Mclsaac, G. F., David, M. B., Gertner, G. Z., & Goolsby, D. A. (2002). Relating net nitrogen input in the Mississippi River basin to nitrate flux in the Lower Mississippi River: A comparison of approaches. *Journal of Environmental Quality*, *31*(5), 1610–1622. https://doi.org/10.2134/jeq2002.1610

Mellander, P. E., Jordan, P., Melland, A. R., Murphy, P. N. C., Wall, D. P., Mechan, S., et al. (2013). Quantification of phosphorus transport from a karstic agricultural watershed to emerging spring water. *Environmental Science and Technology*, *47*(12), 6111–6119. https://doi.org/10.1021/es304909y

Pellerin, B. A., Bergamaschi, B. A., Downing, B. D., Saraceno, J. F., Garrett, J. D., & Olsen, L. D. (2013). Optical techniques for the determination of nitrate in environmental waters: Guidelines for instrument selection, operation, deployment, maintenance, quality assurance, and data reporting, U.S. Geological Survey Techniques and Methods 1–D5.

Pellerin, B. A., Bergamaschi, B. A., Gilliom, R. J., Crawford, C. G., Saraceno, J., Frederick, C. P., et al. (2014). Mississippi river nitrate loads from high frequency sensor measurements and regression-based load estimation. *Environmental Science and Technology*, *48*(21), 12,612–12,619. https://doi.org/10.1021/es504029c

Pellerin, B. A., Saraceno, J. F., Shanley, J. B., Sebestyen, S. D., Aiken, G. R., Wollheim, W. M., & Bergamaschi, B. A. (2012). Taking the pulse of snowmelt: In situ sensors reveal seasonal, event and diurnal patterns of nitrate and dissolved organic matter variability in an upland forest stream. *Biogeochemistry*, *108*(1–3), 183–198. https://doi.org/10.1007/s10533-011-9589-8

Prior, J. (1991). *Landforms of Iowa* (1st ed.). Iowa City, IA: University of Iowa Press.

Pryor, S. C., Barthelmie, R. J., & Schoof, J. T. (2013). High-resolution projections of climate-related risks for the Midwestern USA. *Climate Research*, *56*(1), 61–79. https://doi.org/10.3354/cr01143

Rabalais, N. N., Turner, R. E., Gupta, B. K., Boesch, D. F., Chapman, P., & Murrell, M. C. (2007). Hypoxia in the northern Gulf of Mexico: Does the science support the plan to reduce, mitigate, and control hypoxia? *Estuaries and Coasts*, *30*(5), 753–772. https://doi.org/10.1007/BF02841332

Rabalais, N. N., Turner, R. E., & Wiseman, W. J. (2002). Gulf of Mexico hypoxia, a.k.a. "The Dead Zone". *Annual Review of Ecology and Systematics*, *33*(1), 235–263. https://doi.org/10.1146/annurev.ecolsys.33.010802.150513

Randall, G. W., & Mulla, D. J. (1995). Nitrate nitrogen in surface waters as influenced by climatic conditions and agricultural practices. *Journal of Environmental Quality*, *30*(2), 337–344.
Rode, M., Halbedel Née, S., Angelstein, M. R., Anis, D. B., & Weitere, M. (2016). Continuous in-stream assimilatory nitrate uptake from high-frequency sensor measurements. *Environmental Science and Technology*, *50*(11), 5685–5694. https://doi.org/10.1021/acs.est.6b00943
Sandhu, D., Singh, A., Fan, N., Wang, D., & Duranceau, S. J. (2016). Hydro-geomorphic response of Everglades to changing climate and anthropogenic activities. *Journal of Hydrology*, *543*, 861–872. https://doi.org/10.1016/j.jhydrol.2016.11.004
Saupe, D. (1988). In H. O. Peitgen & D. Saupe (Eds.), *The science of fractal images*. New York: Springer.
Schilling, K. E., & Helmers, M. (2008). Tile drainage as karst: Conduit flow and diffuse flow in a tile-drained watershed. *Journal of Hydrology*, *349*(3–4), 291–301. https://doi.org/10.1016/j.jhydrol.2007.11.014.
Sebilo, M., Mayer, B., Nicolardot, B., Pinay, G., & Mariotti, A. (2013). Long-term fate of nitrate fertilizer in agricultural soils. *Proceedings of the National Academy of Sciences of the United States of America*, *110*(45), 1–5. https://doi.org/10.1073/pnas.1305372110
Singh, A., Foufoula-Georgiou, E., Porté-Agel, F., & Wilcock, P. R. (2012). Coupled dynamics of the co-evolution of gravel bed topography, flow turbulence and sediment transport in an experimental channel. *Journal of Geophysical Research*, *117*, F04016. https://doi.org/10.1029/2011JF002323
Singh, A., & A. T. Hansen (2018). Gap-filled USGS sensor data for nitrate, discharge and temperature for selected sites in Iowa, USA. Retrieved from the Data Repository for the University of Minnesota. https://doi.org/10.13020/D6T106
Singh, A., Lanzoni, S., Wilcock, P. R., & Foufoula-Georgiou, E. (2011). Multiscale statistical characterization of migrating bed forms in gravel and sand bed rivers. *Water Resources Research*, *47*, W12526. https://doi.org/10.1029/2010WR010122
Sinha, E., Michalak, A. M., & Balaji, V. (2017). Eutrophication will increase during the 21st century as a result of precipitation changes. *Science*, *357*(6349), 405–408. https://doi.org/10.1126/science.aan2409
Sobota, D. J., Compton, J. E., & Harrison, J. A. (2013). Reactive nitrogen inputs to US lands and waterways: How certain are we about sources and fluxes? *Frontiers in Ecology and the Environment*, *11*(2), 82–90. https://doi.org/10.1890/110216
Sprague, L. A., Hirsch, R. M., & Aulenbach, B. T. (2011). Nitrate in the Mississippi River and its tributaries, 1980 to 2008: Are we making progress? *Environmental Science and Technology*, *45*(17), 7209–7216. https://doi.org/10.1021/es201221s
Stoica, P., & Moses, R. L. (1997). *Introduction to spectral analysis*. Upper Saddle River, NJ: Prentice Hall.
Sudduth, E. B., Perakis, S. S., & Bernhardt, E. S. (2013). Nitrate in watersheds: Straight from soils to streams? *Journal of Geophysical Research: Biogeosciences*, *118*, 291–302. https://doi.org/10.1002/jgrg.20030
Tilman, D., Cassman, K. G., Matson, P. A., Naylor, R., & Polasky, S. (2002). Agricultural sustainability and intensive production practices. *Nature*, *418*(6898), 671–677. https://doi.org/10.1038/nature01014
Turner, R. E., Rabalais, N. N., & Justic, D. (2008). Gulf of Mexico hypoxia: Alternate states and a legacy. *Environmental Science and Technology*, *42*(7), 2323–2327. https://doi.org/10.1021/es071617k
U.S. Department of Agriculture (2014). USDA National Agricultural Statistics Service Cropland Data Layer. Published crop-specific data layer [Online] USDA-NASS, Washington, DC. Retrieved from https://nassgeodata.gmu.edu/CropScape/, (accessed May 15, 2017).
Van Meter, K. J., Basu, N. B., Veenstra, J. J., & Burras, C. L. (2016). The nitrogen legacy: Emerging evidence of nitrogen accumulation in anthropogenic landscapes. *Environmental Research Letters*, *11*(3). https://doi.org/10.1088/1748-9326/11/3/035014
Vitousek, P. M., Aber, J. D., Howarth, R. W., Likens, G. E., Pamela, A., Schindler, D. W., et al. (1997). Human alteration of the global nitrogen cycle: Sources and consequences. *Ecological Applications*, *7*(3), 737–750.
von Storch, H., & Zwiers, F. W. (2003). *Statistical analysis in climate research*, Cambridge, England: Cambridge University Press.
Wagenhoff, A., Clapcott, J. E., Lau, K. E. M., Lewis, G. D., & Young, R. G. (2017). Identifying congruence in stream assemblage thresholds in response to nutrient and sediment gradients for limit setting. *Ecological Applications*, *36*(1), 178–194. https://doi.org/10.1002/eap.1457
Wagner, R., Boulger, Jr, R., Oblinger, C., & Smith, B. (2006). Guidelines and standard procedures for continuous water-quality monitors: Station operation, record computation, and data reporting, U.S. Geological Survey Techniques and Methods 1–D3.
Weary, D. J., & Doctor, D. H. (2014). Karst in the United States: A digital map compilation and Database, United States Geological Survey Open-File Report, 1156, 23. https://doi.org/10.3133/ofr20141156
Wetzel, R. G. (2001). *Limnology, lakes and river ecosystems*. San Diego, CA: Academic Press.